Published in final edited form as:
J Heat Transfer. 2010 June ; 132(6): . doi:10.1115/1.4000750.

Heat Transport Capability and Fluid Flow Neutron Radiography of Three-Dimensional Oscillating Heat Pipes

B. Borgmeyer,
Department of Mechanical and Aerospace Engineering, University of Missouri-Columbia, Columbia, MO 65201

C. Wilson,
Department of Mechanical and Aerospace Engineering, University of Missouri-Columbia, Columbia, MO 65201

R. A. Winholtz,
Department of Mechanical and Aerospace Engineering, University of Missouri-Columbia, Columbia, MO 65201

H. B. Ma[1] **[LaPierre Professor]**,
Department of Mechanical and Aerospace Engineering, University of Missouri-Columbia, Columbia, MO 65201

D. Jacobson,
National Institute of Standards and Technologies, 100 Bureau Drive, Gaithersburg, MD 20899

D. Hussey
National Institute of Standards and Technologies, 100 Bureau Drive, Gaithersburg, MD 20899

Abstract

An experimental investigation into the parameters affecting heat transport in two three-dimensional oscillating heat pipes (OHPs) was implemented. A three-dimensional OHP is one in which the center axis of the circular channels containing the internal working fluid do not lie in the same plane. This novel design allows for more turns in a more compact size. The OHPs in the current investigation is made of copper tubings (3.175 mm outside diameter, 1.65 mm inside diameter) wrapped in a three-dimensional fashion around two copper spreaders that act as the evaporator and condenser. The two OHPs have 10 and 20 turns in both the evaporator and condenser. The 20-turn OHP was filled to 50% of the total volume with a high performance liquid chromatography grade water. Transient and steady state temperature data were recorded at different locations for various parameters. Parameters such as heat input, operating temperature, and filling ratio were varied to determine its effect on the overall heat transport. Neutron radiography was simultaneously implemented to create images of the internal working fluid flow at a rate of 30 frames per second. Results show the average temperature drop from the evaporator to condenser decreases at higher heat inputs due to an increase in temperature throughout the

[1]Corresponding author. Present address: Department of Mechanical and Aerospace Engineering, University of Missouri-Columbia, Columbia, MO 65211, mah@missouri.edu.
Contributed by the Heat Transfer Division of ASME for publication in the JOURNAL OF HEAT TRANSFER.

condenser region due to greater oscillations. These large oscillations were visually observed using neutron radiography. As the operating temperature is increased, the thermal resistance is reduced. A decrease in filling ratio tends to create more steady fluid motion; however, the heat transfer performance is reduced.

Keywords

oscillating heat pipe; heat transfer; fluid flow; neutron radiography

1 Introduction

Oscillating heat pipes (OHPs) have become widely investigated due to their capability to transfer large amounts of heat. Oscillating heat pipes are a two phase heat transfer device that transfers heat through oscillating fluid flow. In an OHP, a channel is partially filled with an internal working fluid at saturated conditions. If the tube has a small enough diameter, then surface tension forces overcome gravitational forces and the liquid and vapor form distinct plugs and slugs, respectively. In order to create the distinct plugs and slugs, the maximum tube diameter can be calculated by $D_{\max} = 1.84\sqrt{\sigma / g(\rho_l - \rho_v)}$ where 1.84 is the critical Bond number. By creating the tube inner diameter small enough based on this equation, the vapor and liquid flow in the tube flow in the same direction, which avoids entrainment limits as seen in conventional heat pipes. Applying heat to one end and removing heat from the other creates temperature gradients, which result in pressure differences that when coupled with vapor expansion and contraction cause oscillating fluid flow between the evaporator and condenser regions.

There are many parameters that affect the heat transport in an OHP. The structural parameters, such as the tube size, length, number of turns, and closed or open looped, significantly influence the oscillating motion and heat transfer performance. While the unlooped OHP, in which the working fluid is unable to circulate, can produce the oscillating motion, the closed looped OHP, in which the channel forms a complete loop, has a better heat transfer performance [1]. The number of serpentine turns also affects the overall performance. As the number of turns in a given range increases, the overall heat transfer performance of the OHP increases [2]. The functional parameters such as working fluid, heat input, orientation, and operating temperature also play important roles in an OHP. Khandekar et al. [3] discussed the properties of working fluids and how they aid or inhibit the performance of the OHP. A high pressure gradient due to the temperature gradient produces the pumping action of the OHP. This is desired because it is this pressure difference that allows the working fluid to flow without the aid of a mechanical pump or the use of wick structures as in conventional heat pipes. Khandekar and Groll [4] stated that low heat inputs are unable to generate sufficient pressure perturbations resulting in a lack of pumping action, which is necessary for optimal performance. Charoensawan et al. [2] conducted an experimental investigation into the effects of device orientation on heat transfer performance. Operating temperature was investigated by Ma et al. [5] and they noted that an increase in operating temperature results in reduced temperature drops. All these investigations have been focused on the two-dimensional OHPs, which cannot transfer

heat with a higher heat flux. In addition, for a two-dimensional OHP, it is not easy to produce the bulk circulation due to the turn number limitation in a given heating area.

In the current investigation, two new three-dimensional OHPs have been conducted experimentally and examined the effects of certain parameters such as turn number, operating temperature, charging ratio, and power input in order to develop an OHP that removes heat with a higher heat flux level. In addition to understanding the parameters' effect on heat transfer capabilities, it is also necessary to determine fluid flow characteristics associated with the temperature oscillations. A number of experimental investigations have been conducted utilizing glass tubing to visually track fluid motion within OHPs [6,7]. Due to the low thermal conductivity of glass, it is more difficult to simultaneously monitor temperature with slug flow. The investigation presented herein uses neutron radiography, which allows for fluid flow visualizations at a rate of 30 frames per second (fps) while recording temperature data at several locations.

2 Experiment Setup and Procedure

The OHPs shown in Figs. 1(*a*)–1(*c*), 2(*a*), and 2(*b*) were constructed from copper tubings with outer and inner diameters of 3.175 mm and 1.65 mm, respectively. The evaporator and condenser were constructed from copper blocks. Semicircular channels were milled into the copper blocks to create maximum contact between the two regions and the tubing. The condenser regions have holes dilled through the center for water bath controlled condenser temperature. Similarly, holes were drilled in the evaporator to hold cylindrical cartridge heaters that would serve as the controlled heat input. The copper tubing was laid in the semicircular channels of the evaporator and condenser blocks. Thermal paste was also added to the grooves to reduce contact resistance. The copper block attaching with the copper tubing for the 20-turn OHP has an evaporator section and condenser section of $7.62\times8.89\times2.54\ cm^3$. The length of the adiabatic section was set at 10.16 cm for the 20-turn OHP. In order to achieve a higher heat flux, the 10-turn OHP was designed to be smaller with dimensions of $3.81\times7.62\times2.54\ cm^3$ for the evaporator and $6.35\times7.62\times2.54\ cm^3$ for the condenser. The adiabatic section was set to a length of 7.62 cm. The tubing for the 10-turn OHP was staggered to achieve a clearer image of the fluid flow.

Both OHPs were backfilled to a given charging ratio with a high performance liquid chromatography (HPLC) grade water using a vacuum pump. The OHP was then sealed to maintain sub-atmospheric pressure conditions. 400 W cartridge heaters were covered in thermal paste and inserted into the holes. Cooling bath water was passed through a heat exchanger to control the temperature of the deuterium oxide (^2H_2O) circulating in a separate loop through the OHP. The deuterium oxide (also known as heavy water) does not scatter as many neutrons as water; therefore, images in the condenser region can be recorded more clearly. T thermocouples were placed in different locations in the evaporator, adiabatic, and condenser regions. Prior to experimentation, thermocouples were calibrated to a maximum error of ±0.25°C. The locations for the thermocouples are shown in Figs. 2(*a*) and 2(*b*). The thermocouples were connected to a National Instruments[2] data acquisition (DAQ) system and a personal computer for temperature recording, as shown in Fig. 3. The DAQ system was relayed to record data at the moment the neutron imaging software was initiated to

capture images. This allowed for simultaneous visual and temperature data. The neutron imaging setup, as shown in Fig. 4, was developed at the National Institute of Standards and Technologies' (NIST) research reactor. In this system, the OHP is bombarded with neutrons from the reactor and the hydrogen in the HPLC grade water scatters the neutrons, while a neutron detector downstream from the reactor records the image. The scattering of the neutrons by the water creates a darker image than where there is no water in the OHP. The detector has the capability of recording images at a rate of 30 fps and its resolution is based on neutron flux, OHP material and inner channel diameter, and location from the sensor.

A Staco power supply was wired in parallel with the cartridge heaters and a multimeter to accurately gauge the input power. The entire OHP was surrounded with insulation material to prevent heat transfer with the environment. The insulation was then covered with aluminum foil to prevent airborne radiological contamination. The 20-turn OHP was set up in only the vertical position with bottom heating, whereas the 10-turn was only arranged in the horizontal position. Two condenser settings (20°C and 60°C) were tested at numerous heat inputs for the 20-turn OHP, while only one setting (60°C) was tested for the 10-turn OHP due to time constraints at the NIST. Heat input was increased by increments of 50 W from 0 W to 400 W for the 20-turn OHP. Due to the smaller size and fewer turns for the 10-turn, heat input was incremented by 25 W from 0 W to 100 W and by 50 W from 100 W to 200 W. Temperature data and neutron images were recorded during both the initial increase in heat input (transient) and when the temperatures in all three regions fluctuated about an average value (steady state). Each heat pipe was allowed to cool to room temperature and temperature data and neutron imaging was recorded for a step input from zero to the maximum heat input. Recordings were also taken during shut down from the maximum heat input.

3 Results and Discussion

The experiments were conducted to determine the effect of turn number, heat input, operating temperature, and filling ratio on the heat transfer performance. Using the neutron images, the circulation and oscillating motion occurring in the OHP can be readily observed including flow patterns. The OHPs developed herein performed well overall and the frequency and amplitude of temperature oscillations were very consistent, especially at higher heat fluxes where sustained oscillations and bulk circulation occurred. The consistency of amplitude and frequency of the 20-turn OHP is greater than the 10-turn in general

3.1 20-Turn OHP.

The 20-turn OHP was tested in the vertical position (bottom heating) for heat inputs up to 400 W. Because semicircular channels were milled into the copper block to create maximum contact between the heating block and the tubing, the contact area between the copper block and the tubing can be found as 152.0 cm^2. The calculated area is based on half

[2]Certain trade names and company products are mentioned in the text or identified in an illustration in order to adequately specify the experimental procedure and equipment used. In no case does such identification imply recommendation or endorsement by the National Institute of Standards and Technology, nor does it imply that the products are necessarily the best available for the purpose

the circumference of the tubing times evaporator length time the number of semicircular grooves. Given this contact area, the heat flux level reached at a heat input of 400 W is 2.63 W/cm^2. Two condenser settings of 20°C and 60°C were tested to determine operating temperature effect.

3.1.1 Heat Input Effect.—From the experiments and neutron images conducted in this investigation, there appears to be three stages of fluid flow associated with this novel three-dimensional OHP. The first stage occurs at startup (0–50 W). This stage is shown thermally by a gradual increase in evaporator and adiabatic temperature with a steady condenser temperature. Figure 5 shows the temperature data associated with the startup period. The temperature data shows a steady curve; however, the neutron images show small movements. Also, at the low heat inputs, the growing vapor plugs in the evaporator slowly push the liquid slugs to the condenser. Further increase in heat input creates sufficient unsteady vapor growth required to develop pressure perturbations necessary for fluid exchange between adjacent turns.

The second stage of fluid flow in the OHP is intermittent flow starting at about 50 W up to 150 W for the 20-turn OHP investigated herein. This is where the fluid exchange between the evaporator and condenser regions is occasionally hindered. The stoppage in fluid exchange corresponds to a short steady increase in temperature following sustained temperature oscillations. The stoppage in fluid flow resumes once the temperature difference has increased enough to provide sufficient driving force to transfer the fluid. Figure 6 shows a large stoppage in fluid motion between the time 60–80 s that corresponds to a large increase in temperature. Results shown in Fig. 6 correspond to the 20-turn OHP in a vertical position (bottom heating) maintaining a heat input of 50 W and a condenser temperature of 60°C. Figure 6 shows that the frequency of temperature oscillation is roughly 0.17 Hz with amplitudes ranging from 2°C to 7°C. The majority of the temperature oscillations have amplitudes around 3°C. Figures 7(*a*)–7(*d*) display the neutron images at four separate points in time. Figures 7(*a*)–7(*c*) are during this period of temperature increase and it can be seen that during this time little movement occurs. At 85 s (Fig. 7(*d*)), we start to see a change in the location of the slugs. As heat input is increased, the intermittent flow becomes more periodic.

The third stage of fluid flow occurs at high heat flux (>150 W) in which there are sustained oscillations and bulk circulation. This stage corresponds to steady fluid flow through the OHP with uniform frequency and amplitude. Figure 8 shows the oscillatory temperature readings associated with a 300 W heat input (1.97 W/cm^2) and a condenser setting of 60°C. At this heat input, consistent bulk circulation can be observed from the neutron images. The frequency of temperature oscillation for this heat input is roughly 0.275 Hz. This indicates an increase in frequency with increases in heat input. The amplitudes of oscillations range from about 2°C to 3°C. The amplitudes of oscillations seem to become more consistent at higher heat inputs. Figures 9(*a*)–9(*d*) display the neutron images at times where the evaporator thermocouple peaks and when it reaches its low point. The circulating flow tends to match the frequency of the temperature data. It should also be noted that at higher heat inputs, the velocities of the liquid slugs exceed the capture rate of the detector. The blurring associated with it makes it difficult to track the fluid meniscus. Figure 10 shows the average

temperature drop from the evaporator to the condenser in the 20-turn OHP for condenser setting of 20°C and 60°C. Temperature drop decreases as the heat input increases due to increased fluid flow.

3.1.2 Operating Temperature Effect.—The neutron images comparing operating temperatures show unnoticeable differences; however, it is clear that oscillations start up more easily given a higher condenser setting. Figure 10 shows a decrease in temperature drop with an increase in condenser setting. Consequently, this means a reduced thermal resistance, as seen in Fig. 11. As expected from the results for the heat input effect, the thermal resistance decreases with increase in power input. In addition to the decrease in thermal resistance with heat input, the performance is enhanced as the condenser setting was raised. This increase in performance is based on the change in fluid properties associated with temperature change. For example, the viscosity of water decreases with an increase in temperature, which would allow for greater fluid motion. There appears to be no discernable differences between the fluid flow images at different condenser settings.

3.2 10-Turn OHP.

The 10-turn OHP was tested in the horizontal position for heat inputs up to 200 W. The contact area for the 10-turn OHP was calculated to be 38.0 cm^2. This corresponds to a maximum heat flux of 5.26 W/cm^2 at a heat input of 200 W. The filling ratio was decreased in situ during the experiments. The first filling ratio was roughly 50% with the two subsequent ratios being less. Exact values are unknown due to the inability to weigh the OHP during the process. However, from the images it was determined that the three filling ratios were roughly 53%, 35%, and 30%, respectively. A startup similar to the 20-turn OHP was noticed. The liquid slugs were slowly forced out of the evaporator section, as shown in Figs. 12(*a*) and 12(*b*). Small oscillation exists until the pressure perturbations are sufficient to force the liquid back into the evaporator (Fig. 12(*c*)).

3.2.1 Filling Ratio Effect.—The filling ratio has an inverse effect on both the fluid motion and heat transfer. The filling ratio of 53% showed good heat transfer; however, at the lower heat input of 50 W (Fig. 13), the fluid motion in hindered by the large mass of fluid. The filling ratio of 35% shows a slightly lower average evaporator temperature than the higher filling ratio. This may be due to the increase in amplitude and frequency of oscillation. Figure 14 shows the increased temperature oscillations for the filling ratio of 35%. A further decrease in filling ratio to 30% results in a large increase in evaporator temperature at the same heat input of 50 W (Fig. 15). Temperature and imaging data suggest an increase in fluid motion in the OHP; however, the reduction in liquid slugs to carry heat from the evaporator to condenser causes an increase in temperature. Also, a decreased filling ratio was noticed to cause the fluid run toward gravity. This causes the majority of the liquid to fill only one side of the OHP, as seen in Figs. 16(*a*)–16(*c*). Figures 16(*a*)–16(*c*) show the typical fluid distribution for the three filling ratios at 50 W (1.32 W/cm^2). Because of this tendency, full circulation through the OHP is hindered and the liquid slug will only oscillate within the same channel or occasionally with the adjacent one. Figures 17 and 18 show the temperature drop and thermal resistance versus heat input for the three filling ratios. There is an obvious decrease in heat transfer performance with the filling ratios less than 53%.

4 Conclusions

An experimental investigation was implemented to determine the heat transfer and fluid flow characteristics of two novel three-dimensional OHP. The effects of filling ratio, turn number, power input, and operating temperature were investigated to determine their effect on heat transport performance. Results show that when the turn number is different, the effect of power input on the heat transfer performance is different. The neutron images show that both oscillating motion and circulation exist when the power input is higher than 150 W for the 20-turn OHP investigated herein. As the power input increases for the 20-turn OHP, the temperature difference between the evaporator and condenser or effective thermal resistance decreases, which is very different from the conventional heat pipe or most of heat transfer devices. When the turn number was reduced to 10, the temperature difference between the evaporator and condenser or the effective thermal resistance is almost constant or increases slightly as the power input increases. In addition, it is found that the frequency for both OHPs increases as the input power increases. The operating temperature significantly affects the heat transfer performance for both OHPs. As the operating temperature increases, the temperature difference or effective thermal resistance decreases for both OHPs. A lower filling ratio results in larger and more frequent fluid motions; however, heat transport capability is reduced. The novel design of this three-dimensional OHP creates a high performance device with consistent frequencies and amplitudes not commonly observed in OHPs.

Acknowledgment

The work presented in this article was funded by the Office of Naval Research under Grant No. N00014-06-1-1119, which was directed by Dr. Mark Spector. The authors would also like to acknowledge the National Institute of Standards and Technology, U.S. Department of Commerce, for providing the neutron research facilities used in this work.

Nomenclature

D	diameter, m
g	gravity, m/s^2
ρ	density, kg/m^3
σ	surface tension, N/m

Subscripts

max	maximum
l	liquid
υ	vapor

References

[1]. Wilson C, Borgmeyer B, Winholtz RA, Ma HB, Jacobson D, and Hussey D, 2008, “Thermal and Visual Observation of Water and Acetone Oscillating Heat Pipes,” ASME Summer Heat Transfer Conference, Jacksonville, FL, Jul. 10–14.

[2]. Charoensawan P, Khandekar S, Groll M, and Terdtoon P, 2003, “Closed Loop Pulsating Heat Pipes Part A: Parametric Experimental Investigations,” Appl. Therm. Eng, 23, pp. 2009–2020.

[3]. Khandekar S, Dollinger N, and Groll M, 2003, “Understanding Operational Regimes of Closed Loop Pulsating Heat Pipes: An Experimental Study,” Appl. Therm. Eng, 23(6), pp. 707–719.

[4]. Khandekar S, and Groll M, 2003, “On the Definition of Pulsating Heat Pipes: An Overview,” Proceedings of the Fifth Minsk International Seminar, Minsk, Belarus.

[5]. Ma HB, Wilson C, Borgmeyer B, Park K, Yu Q, Choi US, and Tirumala M, 2006, “Nanofluid Effect on the Heat Transport Capability in an Oscillating Heat Pipe,” Appl. Phys. Lett, 88(14), p. 143116.

[6]. Xu JL, Li YX, and Wong TN, 2005, “High Speed Flow Visualization of a Closed Loop Pulsating Heat Pipe,” Int. J. Heat Mass Transfer, 48, pp. 3338–3351.

[7]. Khandekar S, Schneider M, Schafer P, Kulenovic R, and Groll M, 2002, “Thermofluid Dynamic Study of Flat-Plate Closed-Loop Pulsating Heat Pipes,” Microscale Thermophys. Eng, 6, pp. 303–317.

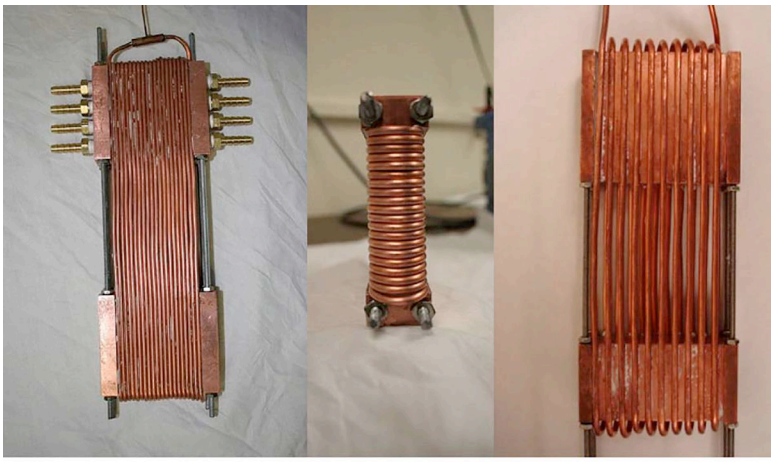

Fig. 1. 20-turn (*a* and *b*) and 10-turn (*c*) OHPs

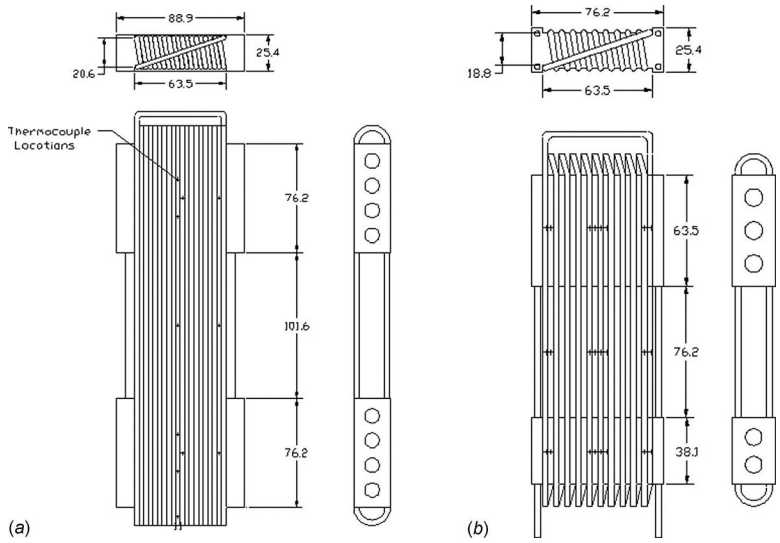

Fig. 2. Dimensions and thermocouple locations for the 20-turn (*a*) and 10-turn (*b*) OHPs (dimensions in mm)

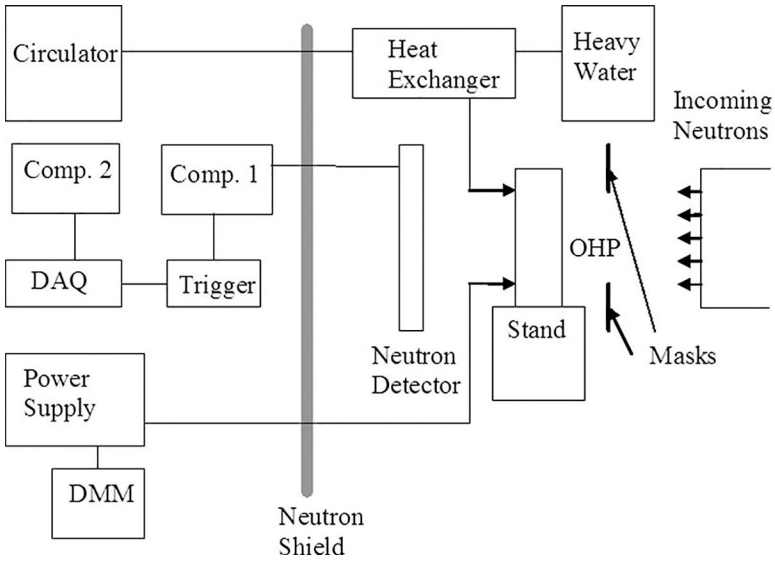

Fig. 3. Experimental setup

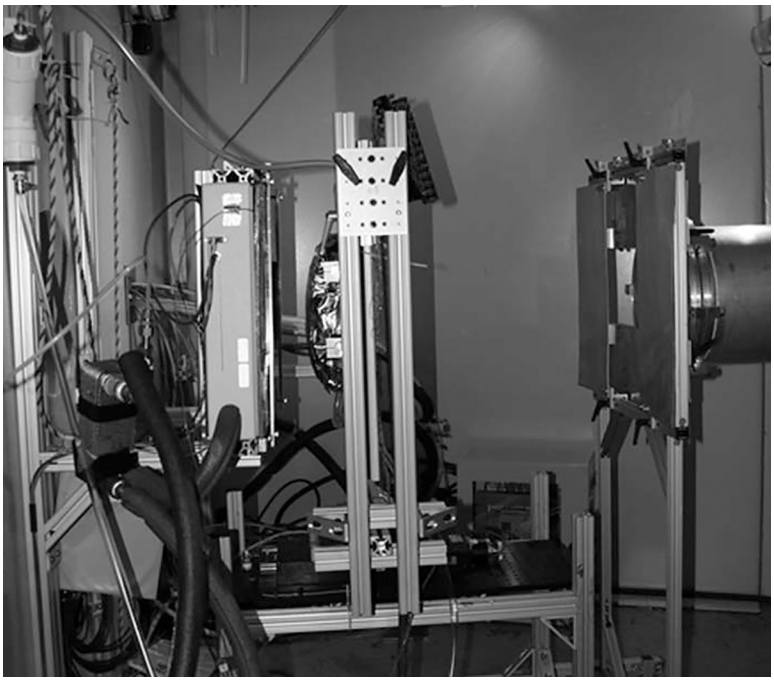

Fig. 4. Neutron imaging setup

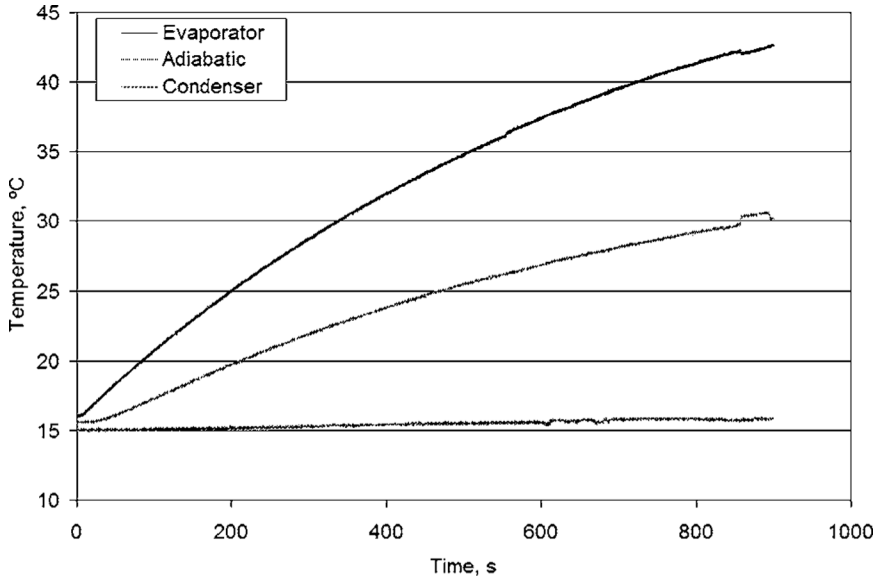

Fig. 5. Temperature data for the startup stage for the 20-turn OHP

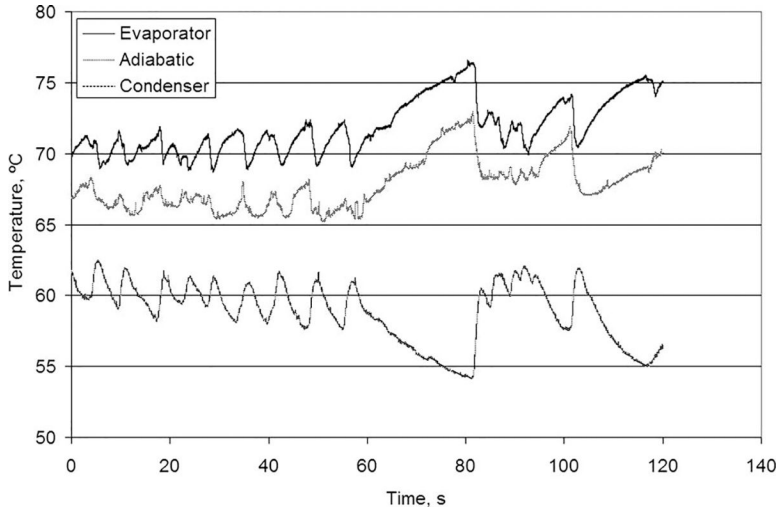

Fig. 6. Temperature data for the intermittent stage for the 20-turn OHP (heat input: 50 W, condenser setting: 60°C)

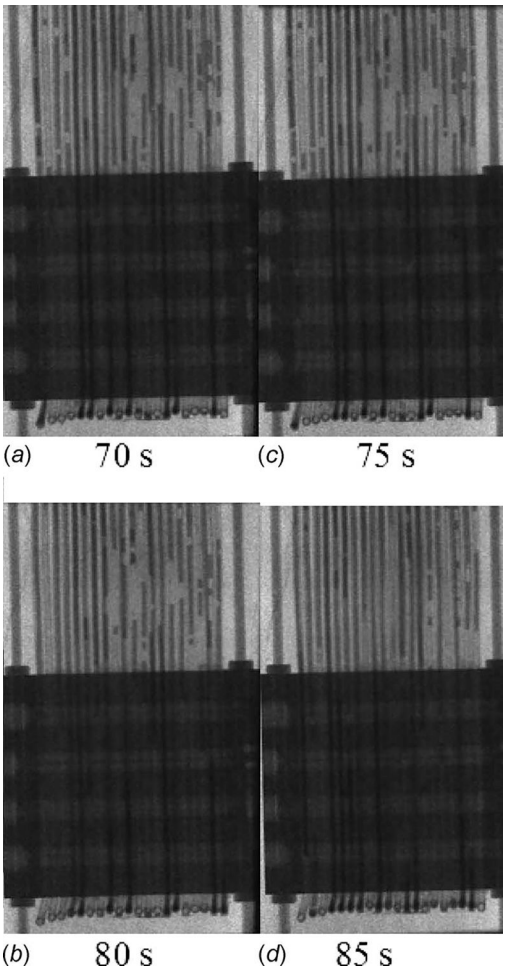

Fig. 7. Neutron images of the intermittent stage for the 20-turn OHP at (*a*) 70 s, (*b*) 75 s, (*c*) 80 s, and (*d*) 85 s

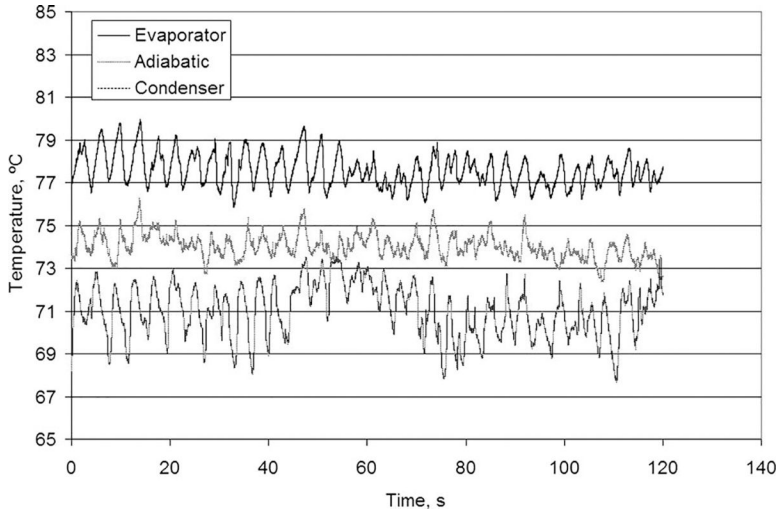

Fig. 8. Temperature data for the bulk circulation stage for the 20-turn OHP (heat input: 300 W, condenser setting: 60°C)

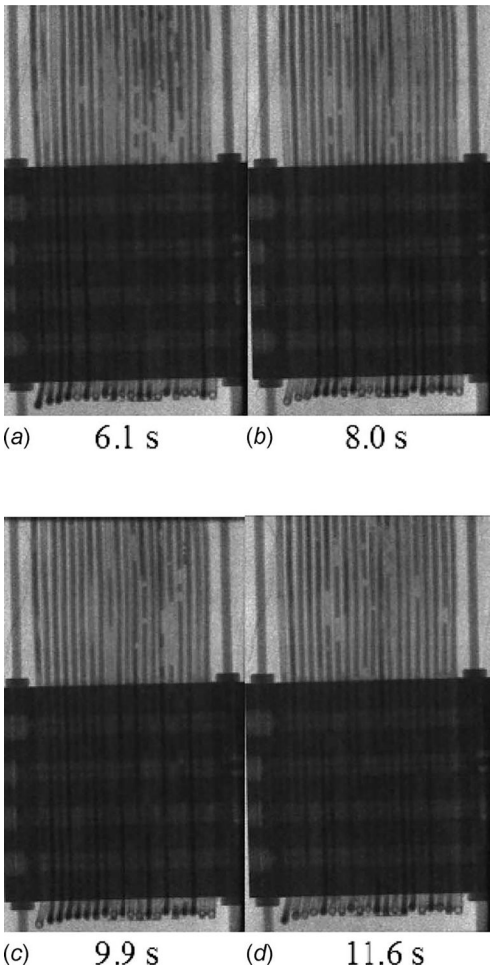

Fig. 9. Neutron images of the circulation stage for the 20-turn OHP at (a) 6.1 s, (*b*) 8.0 s, (*c*) 9.9 s, and (*d*) 11.6 s

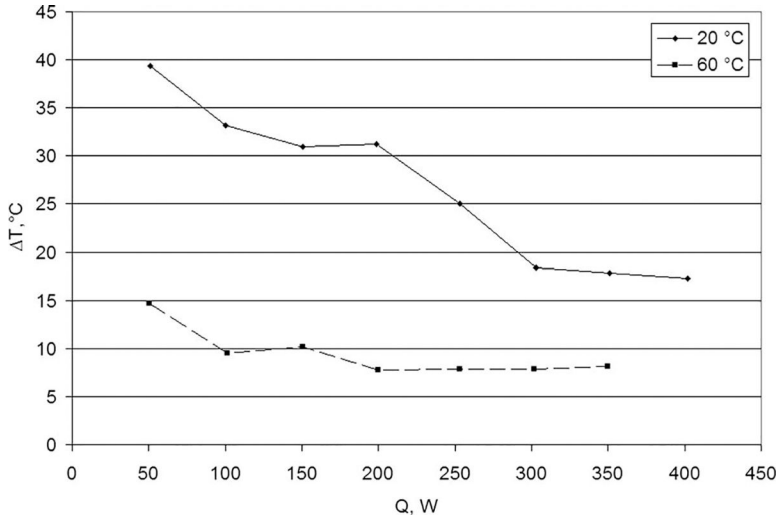

Fig. 10. Temperature drop versus heat flux for the 20-turn OHP

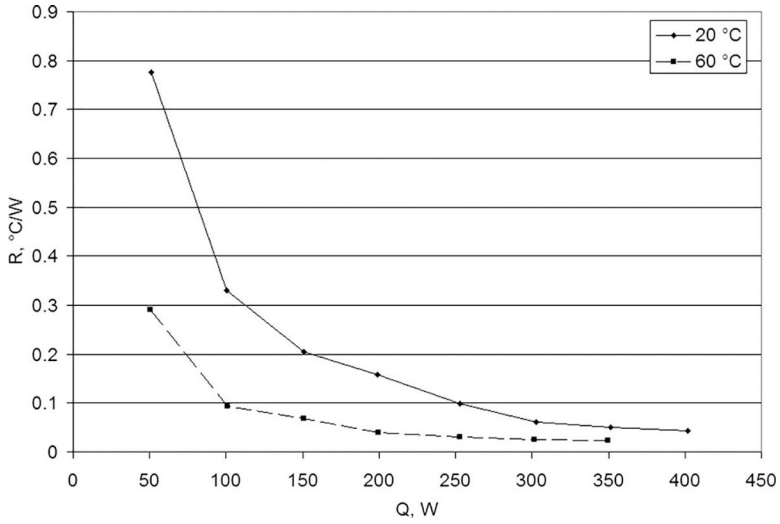

Fig. 11. Thermal resistance versus heat flux for the 20-turn OHP

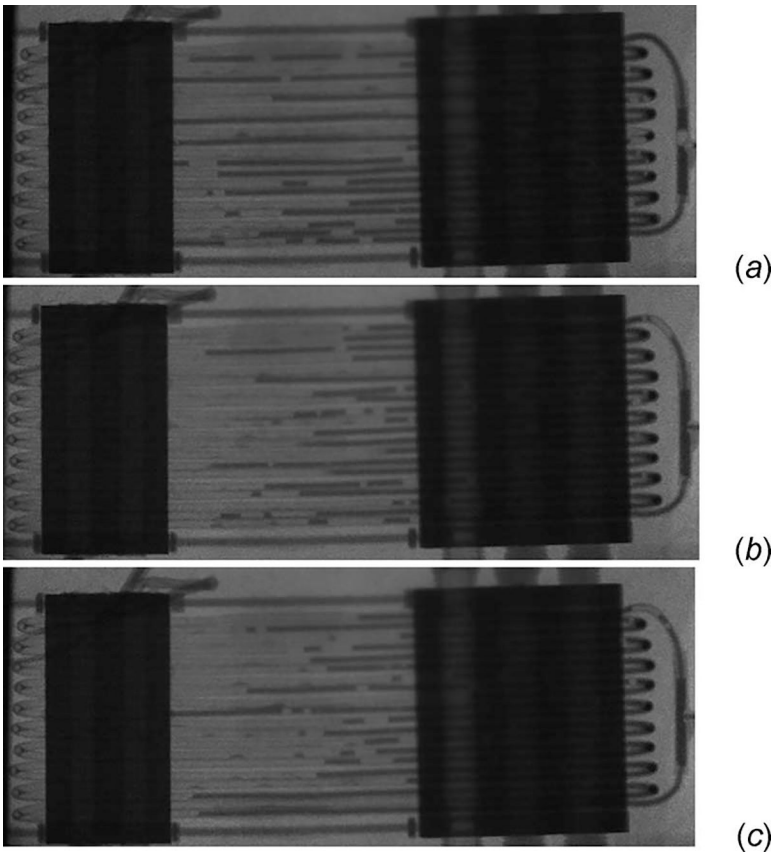

Fig. 12. Startup of the 10-turn OHP at (*a*) 0 s, (*b*) 400 s, and (*c*) 600 s

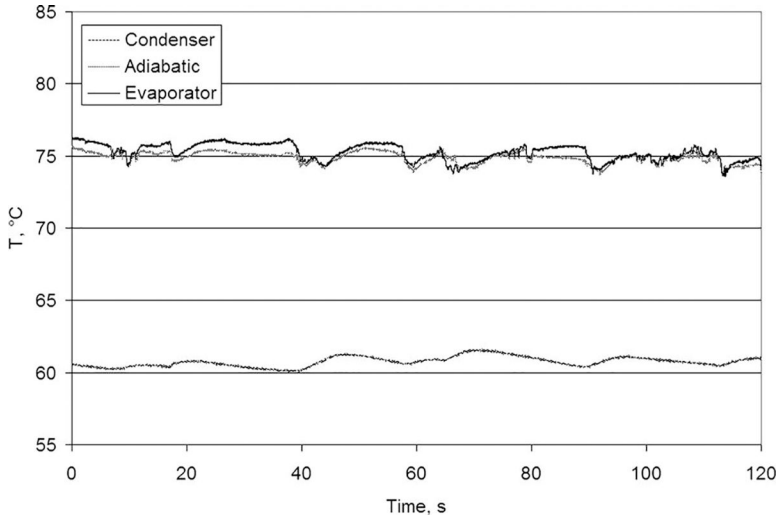

Fig. 13. Temperature fluctuations at a filling ratio of 53% for the 10-turn OHP

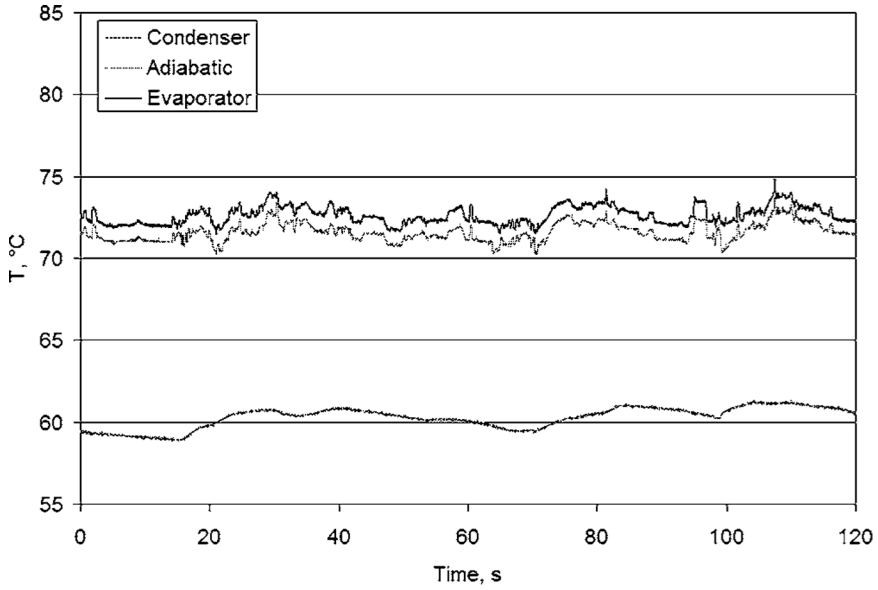

Fig. 14. Temperature fluctuations at filling ratio of 35% for the 10-turn OHP

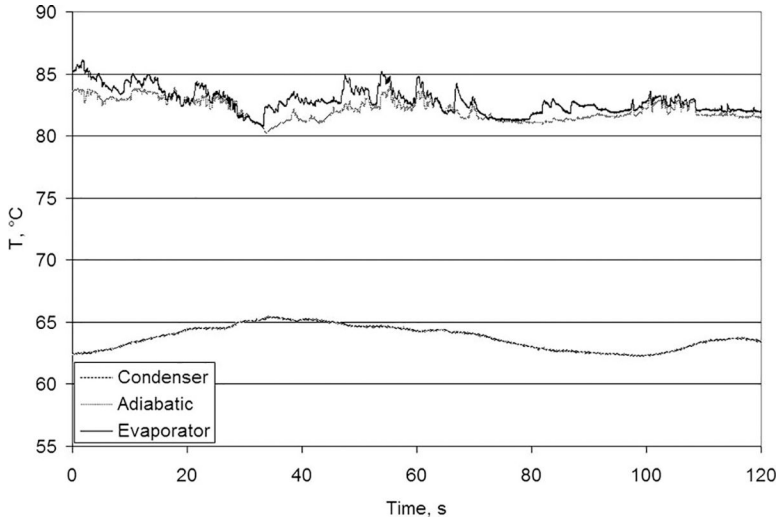

Fig. 15. Temperature fluctuations at a filling ratio of 30% for the 10-turn OHP

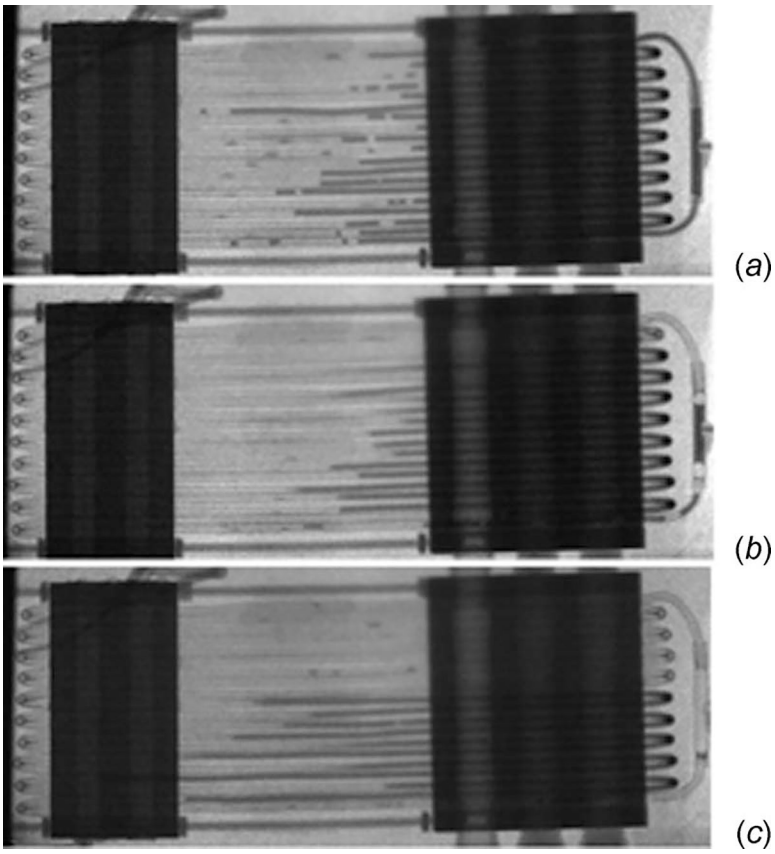

Fig. 16. Typical fluid distribution at low heat input for filling ratio of (*a*) 53%, (*b*) 35%, and (*c*) 30%

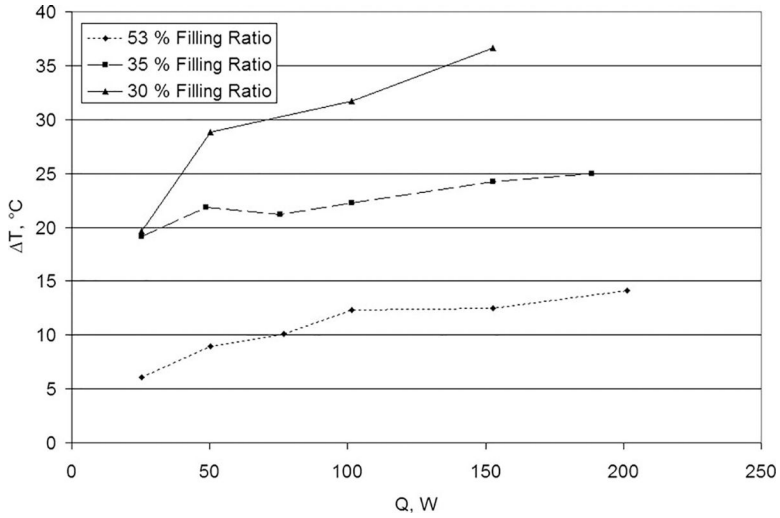

Fig. 17. Temperature drop given different filling ratios for the 10-turn OHP

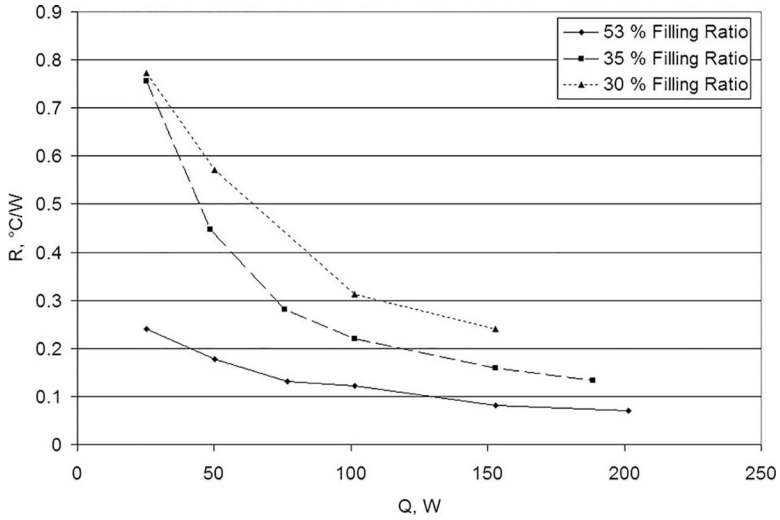

Fig. 18. Thermal resistance given different filling ratios for the 10-turn OHP